Artur Słomski*, Zbigniew Rudy*, Tomasz Bednarski, Piotr Białas, Eryk Czerwiński, Łukasz Kapłon, Andrzej Kochanowski, Grzegorz Korcyl, Jakub Kowal, Paweł Kowalski, Tomasz Kozik, Wojciech Krzemień, Marcin Molenda, Paweł Moskal, Szymon Niedźwiecki, Marek Pałka, Monika Pawlik, Lech Raczyński, Piotr Salabura, Neha Gupta-Sharma, Michał Silarski, Jerzy Smyrski, Adam Strzelecki, Wojciech Wiślicki, Marcin Zieliński and Natalia Zoń

3D PET image reconstruction based on the maximum likelihood estimation method (MLEM) algorithm

Abstract: A positron emission tomography (PET) scan does not measure an image directly. Instead, a PET scan measures a sinogram at the boundary of the field-of-view that consists of measurements of the sums of all the counts along the lines connecting the two detectors. Because there is a multitude of detectors built in a typical PET structure, there are many possible detector pairs that pertain to the measurement. The problem is how to turn this measurement into an image (this is called imaging). Significant improvement in PET image quality was achieved with the introduction of iterative reconstruction techniques. This was realized approximately 20 years ago (with the advent of new powerful computing processors). However, three-dimensional imaging still remains a challenge. The purpose of the image reconstruction algorithm is to process this imperfect count data for a large number (many millions) of lines of response and millions of detected photons to produce an image showing the distribution of the labeled molecules in space.

Keywords: image reconstruction; positron emission tomography.

***Corresponding authors: Artur Słomski and Zbigniew Rudy,** Faculty of Physics, Astronomy and Applied Computer Science, Jagiellonian University, 30-059 Kraków, Reymonta 4 Street, Poland, E-mail: artur.slomski@gmail.com; zbigniew.rudy@uj.edu.pl
Tomasz Bednarski, Piotr Białas, Eryk Czerwiński, Grzegorz Korcyl, Jakub Kowal, Tomasz Kozik, Wojciech Krzemień, Paweł Moskal, Szymon Niedźwiecki, Marek Pałka, Monika Pawlik, Piotr Salabura, Neha Gupta-Sharma, Michał Silarski, Jerzy Smyrski, Adam Strzelecki, Marcin Zieliński and Natalia Zoń: Faculty of Physics, Astronomy and Applied Computer Science, Jagiellonian University, Kraków, Poland
Łukasz Kapłon: Faculty of Physics, Astronomy and Applied Computer Science, Jagiellonian University, Kraków, Poland; and Faculty of Chemistry, Jagiellonian University, Kraków, Poland
Andrzej Kochanowski and Marcin Molenda: Faculty of Chemistry, Jagiellonian University, Kraków, Poland
Paweł Kowalski, Lech Raczyński and Wojciech Wiślicki: Swierk Computing Centre, National Centre for Nuclear Research, Otwock-Swierk, Poland

Introduction

Positron emission tomography (PET) is a fully developed technology used for medical imaging and its importance is still rapidly increasing. There is an established appreciation of the significance of the functional information (as opposed to anatomical obtained, e.g., via X-ray examination) that is provided by PET, in particular its value for the purpose of medical diagnosis and monitoring therapy response. The essential task in PET is to reconstruct a source distribution, that is, to obtain an accurate image of the radioactivity distribution throughout the patient. This is done in order to extract metabolic information about the patient's body. PET imaging is unique in that it shows the chemical functioning of tissues *in vivo*, whereas common imaging techniques, such as X-ray, show the structure of tissues.

The method is as follows: the chosen molecule (ligand) is labeled with a radioactive atom (i.e., a radiotracer is substituted) and a certain amount of the labeled molecules is administered to the patient. The choice depends on the metabolic process of interest. The labeled molecules follow their specific biochemical tracts inside the patient's body. The radioactive atoms (or rather their nuclei) used as labels are unstable β+ emitters and undergo radioactive decay at random directions, leading to the emission of positrons. A positron emitted during the radioactive decay process annihilates with an electron in tissue and as a result a pair of gamma quanta is emitted. The two gamma quanta fly back-to-back, that is,

in opposite directions and can be recorded outside the patient's body by scintillation detectors.

Every detected pair of quanta forms a line of response (LOR). Austrian mathematician Johann Radon [1–3] proved that if such projections are sufficiently numerous, radiation intensity can be reconstructed (this problem is well posed). However, the solution does not have a closed-form expression. Numerical methods are required. Currently, the present approach consists of iterative algorithms derived from the maximum likelihood estimation method (MLEM).

The naïve reconstruction algorithm used to calculate the radioactivity distribution from the projections is based on counting activity. The algorithm adds activity for each pixel along an LOR detected by a detector pair. The process is repeated for all measured LORs, resulting in an image (discretized distribution of radiation intensity) of the original object. This reconstructed image contains streak artifacts and is blurred.

Two-dimensional imaging

Two-dimensional (2D) PET imaging considers only LORs lying within a specified imaging plane. The LORs are organized into sets of projections, that is, line integrals are calculated for all r values for a fixed direction φ (see Figure 1). The collection of all projections as a 2D function of r and φ forms a sinogram in (r, φ) representation. The measured counts in the projection sinogram corresponding to the calculated r are added to the (x, y) pixel in the reconstruction matrix. This is repeated for all projection angles (Figure 1).

It is possible to reconstruct a whole 3D volumetric object by repeating 2D data acquisition for multiple axial (in z direction) slices, although the procedure is tedious. When the sinogram for each value of z is reconstructed, the image planes can be stacked together one after the other to form a three-dimensional (3D) image. Although this can be considered as a form of 3D imaging, it is

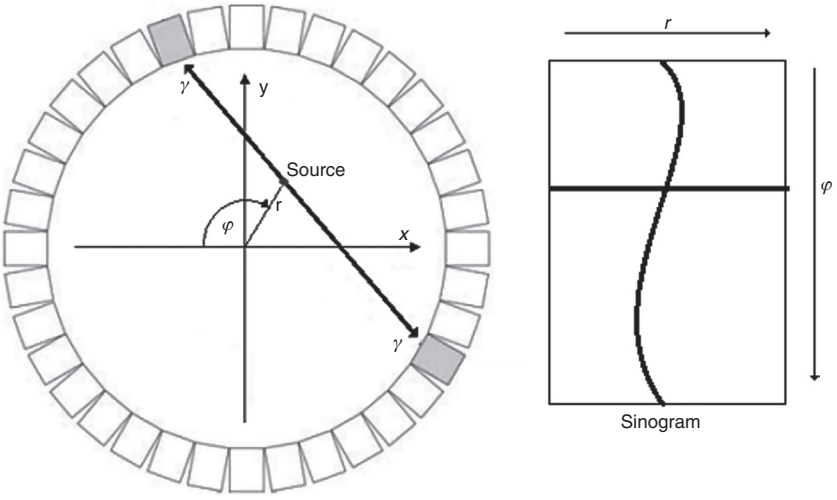

Figure 1 Schematic diagram of PET. Two gamma rays emitted as a result of positron annihilation are detected by two detectors. The lines connecting the detectors (left are described by coordinates (r, φ) and are represented on the sinogram (right).

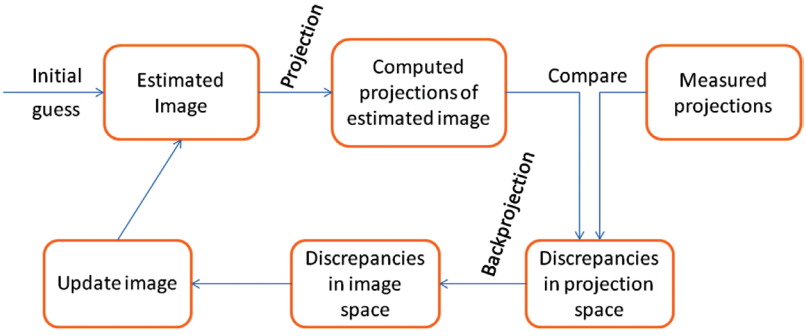

Figure 2 Flow chart of the iterative image reconstruction method.

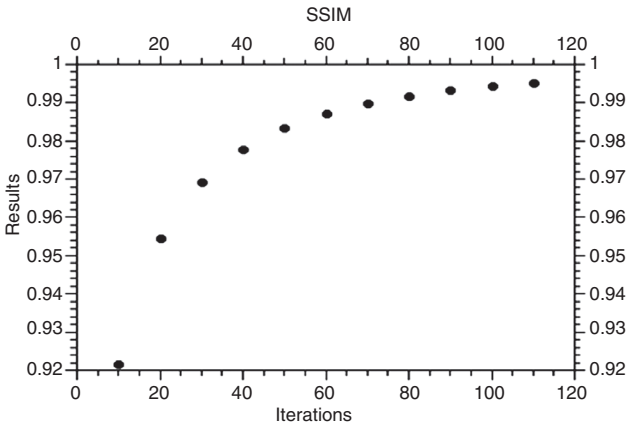

Figure 3 Algorithm convergence proof.
Horizontal, that is, abscissa axis: number of iterations. Vertical, that is, ordinate axis: value of structural similarity metric (SSIM; it measures the spatial correlation between the pixels of the reference and test images to quantify the degradation of the structure of an image, the SSIM value is equal 1 only if two images are identical in considered pixels [6]).

different from the 3D acquisition model described in the following section. There is a handful of effective 2D iterative procedures for imaging [4].

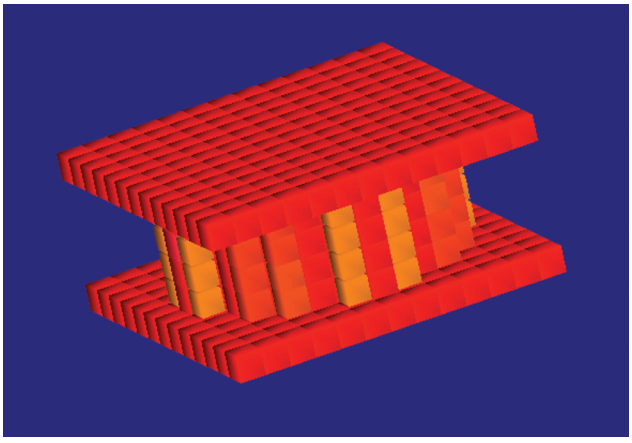

Figure 4 The shape of the original image (phantom).

Three-dimensional imaging

Fully 3D measurements require more storage of data. As a result, reconstruction becomes more computationally intensive. The solution is to use iterative methods such as the MLEM.

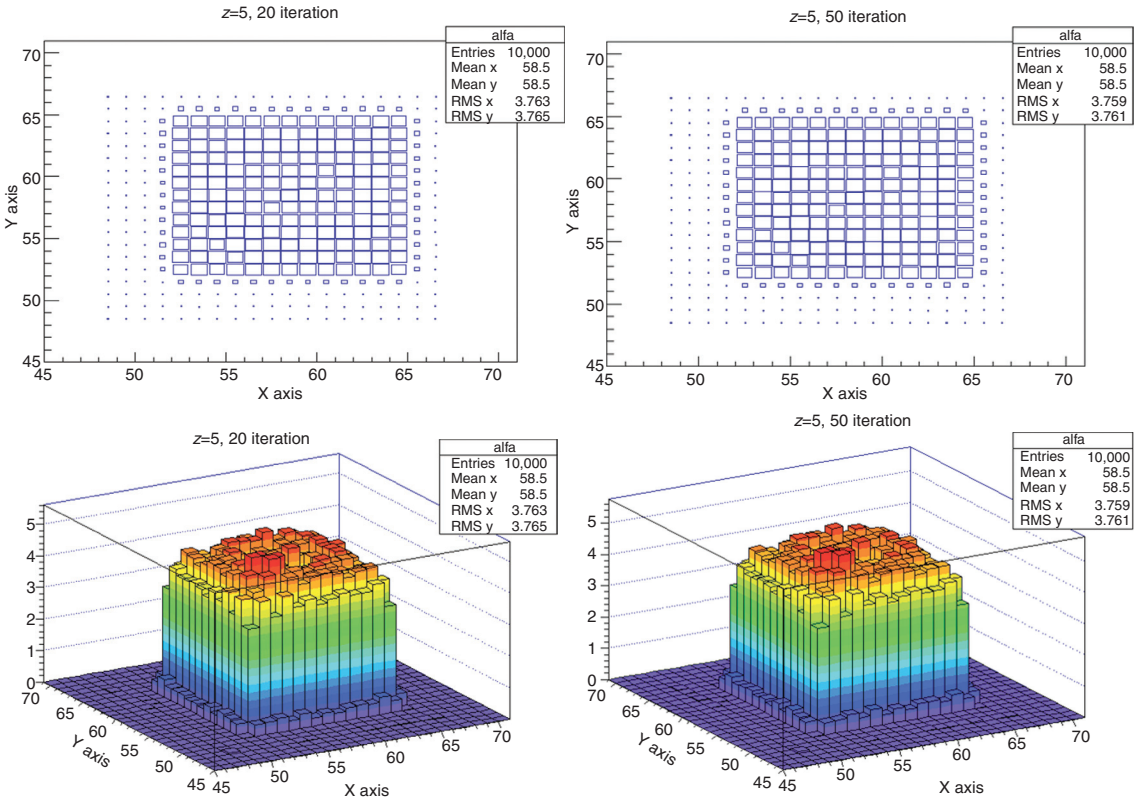

Figure 5 Reconstruction image shown for section at z=5, that is, through the square base of the phantom.
Number of iterations: 20 and 50.

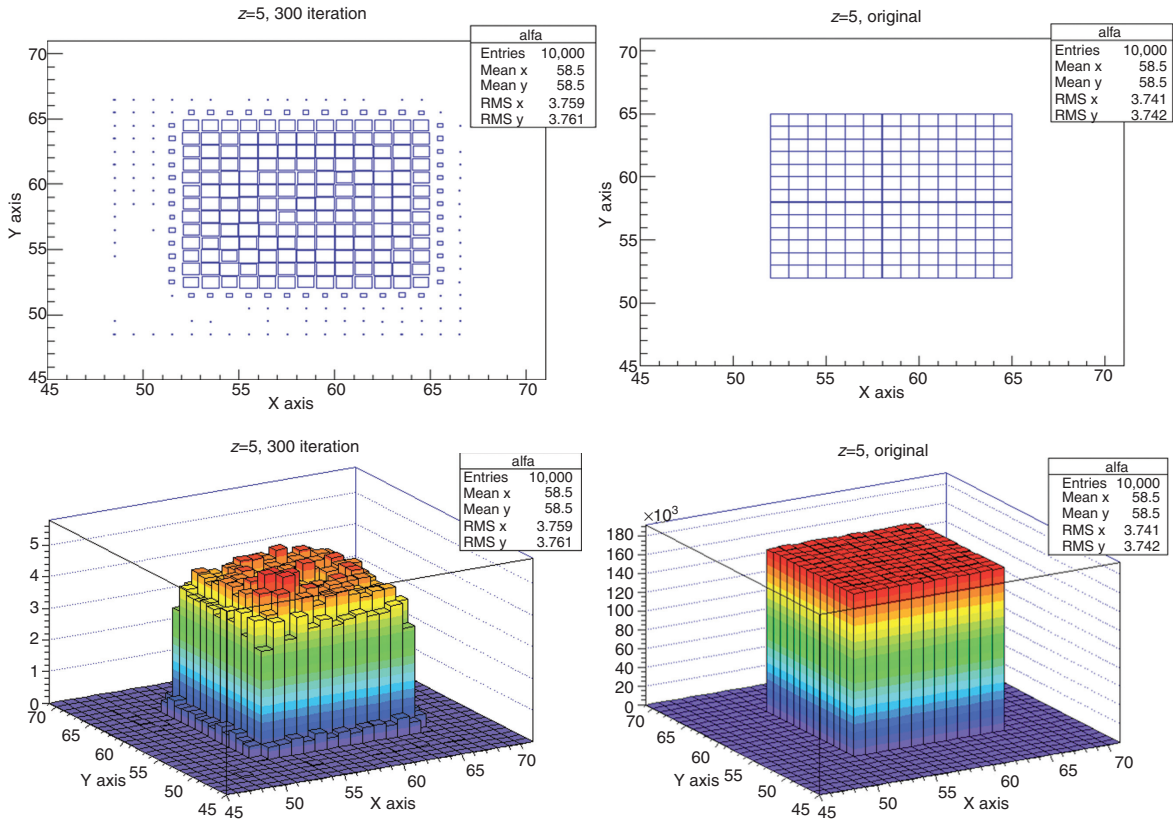

Figure 6 Reconstruction image shown for section at z=5, that is, through the square base of the phantom.
Upper left and lower left part of the figure: result after 300 iterations. Upper right and lower right part of the figure: how the ideal image reconstruction should look like is presented.

The diagram in Figure 2 shows the basic procedure for using an iterative algorithm. The initial estimate of the image in an iterative algorithm is usually a uniform distribution. The projections are computed from the image and compared with the measured projections. If there is a difference between the estimated and measured projections, corrections are made to improve the estimated image, and a new iteration is performed to assess the convergence between the estimated and measured projections. Iterations are continued until a reasonable agreement between the two sets of projections is achieved. The MLEM reconstruction is given as [5]:

$$\lambda_j^{k+1} = \frac{\lambda k}{\sum_i^m C_{ij}} \sum_i^m \frac{C_{ij}}{\sum_j^m C_{ij} \lambda_j^k}$$

where

λ_j^k – value of reconstructed image at the pixel j for the k-th iteration,

k – iteration number,

j – pixel number,

i – the bin number of the projection,

C_{ij} – probability of detecting an emission from the pixel j in bin i of the projection.

In 3D PET imaging, all LORs are acquired in addition to lying on oblique imaging planes. A fully 3D mode is used to increase sensitivity (by means of increasing the number of measured LORs) and thus to lower the statistical noise associated with photon counting improving the signal-to-noise ratio in the reconstructed image. In 3D reconstruction, the projection coordinates must be expanded for another dimension to transform the LOR from (x, y, z) coordinates.

One method to represent a projection for 3D reconstruction (i.e., to label the bins in which measured LORs are counted) is to use the coordinate system of the projection (r, θ, φ, sign wekx, sign weky, sign wekz) where:

r – distance from the origin of the coordinate system,

θ – angle between the LOR and the positive half of axis OZ,

φ – angle between LOR projection onto the xy plane and the negative half of axis OX,

sign wekx – sign of a component x of distance vector r,

sign weky – sign of a component y of distance vector r,

sign wekz – sign of a component z of distance vector r.

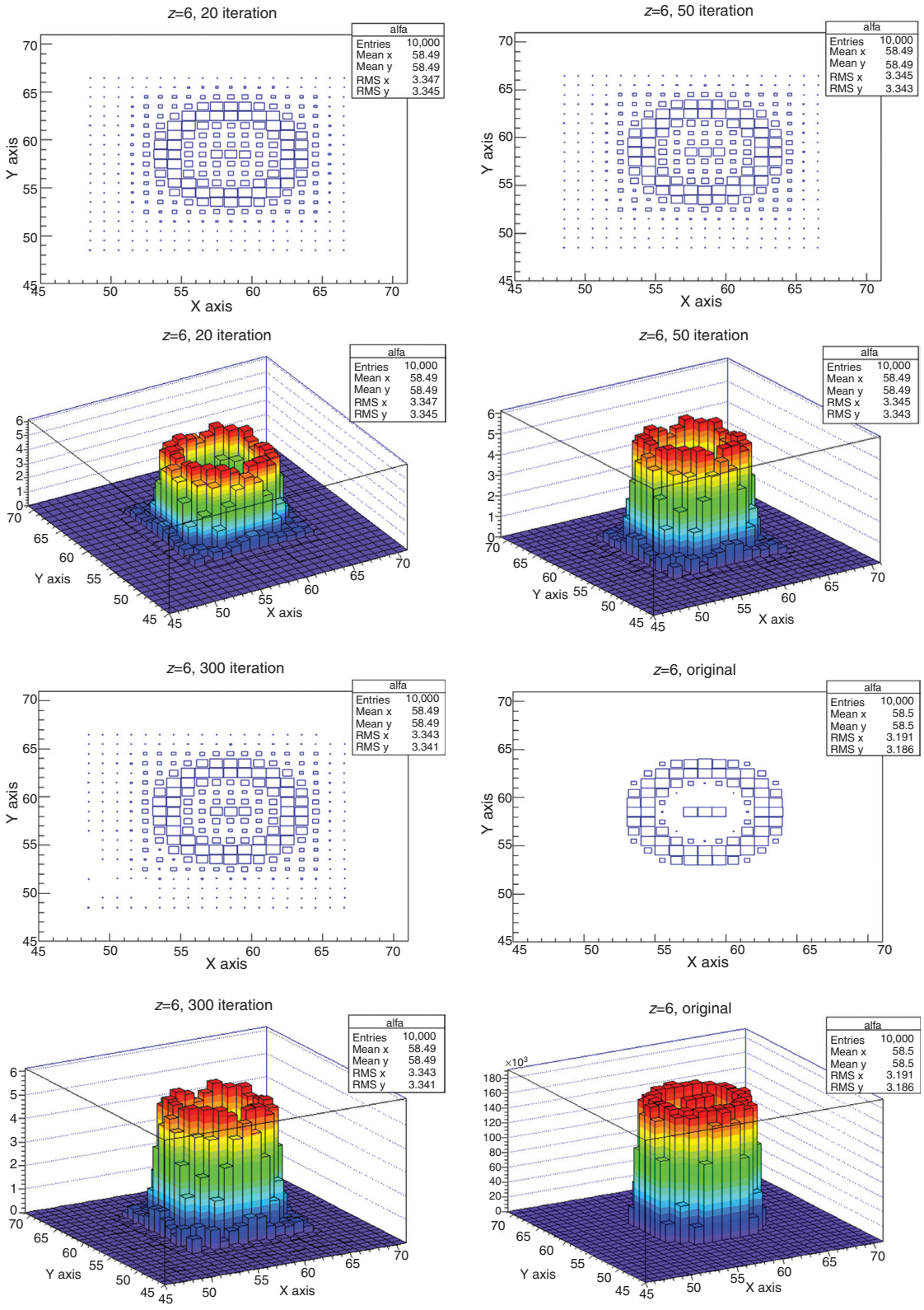

Figure 7 Reconstruction image shown for section at z=6 of the phantom.
Number of iterations: 20, 50, 300. The walls and the central rod of the phantom are reconstructed in a very good manner. Additionally (the plot entitled "original"), how the ideal image reconstruction should look like at z=6 is presented.

The algorithm implemented with the coordinate system of the projection is convergent, as shown in Figure 3, which represents the comparison of images by the structural similarity (SSIM) method depending on the number of iterations (it should be noted that the algorithm works well even though the bins in the projection space are not uniquely described).

Results

Here, examples of algorithm results are shown. Figure 4 presents the original object, that is, the phantom. It is assumed that the phantom radiates uniformly (Monte Carlo simulations were used in order to obtain 100 million LORs). The phantom forms a cylinder placed between two square bases. The bases are slightly larger than the cylinder ring (Figure 4). The cylinder is empty inside with the central rod of the rectangular section connecting the bases. The cylinder is placed in 3D space with the bases parallel to the *xy* plane. Figures 5–7 show the results of the imaging algorithm after 20, 50, and 300 iterations, proving convergence. In fact, the structure of the phantom is reproduced by the imaging algorithm that is steered by simulated data. Cross-sections at different levels of the z coordinate for the reconstruction image are shown, for 2D sections parallel to the *xy* plane (Figure 6) for z=5, that is, the section goes just through the square basis of the cylinder (Figure 7) for z=6, the section shows the walls of the cylinder and the rod in the center.

Conclusions

The presented version of the 3D image reconstruction algorithm, even though it describes the bins of the projection space only approximately (projection space stores information about accumulated LORs), works very well. Further, it quickly reaches an advanced degree of convergence.

With regard to statistical reconstruction methods, the success of the presented algorithm enables us to state that statistical reconstruction methods seem to be a reasonable choice. Many assumptions about the noise can be made, but for the emission data the Poisson model (with regard to properties of distribution of emission) seems to be most adequate.

An appealing feature of the presented iterative (update) equations is that the positivity constraint is automatically fulfilled (in the reconstructed image, its pixels in the radiation space should not have an intensity value <0). It should be noted that the presented algorithm is very resistant in the case when part of the gamma detectors, for any reason, is off; only LORs that were measured influence the result of the algorithm; signal-to-ratio may suffer, but no artifacts are formed.

It is often claimed that expectation maximization methods have drawbacks, such as noisy images are obtained from over-iterated reconstructions (an over-iterated reconstruction may happen if the unwieldy stopping rule is used). However, this version of the expectation maximization based algorithm is free from such unwanted activities.

Acknowledgments: We acknowledge technical and administrative support from M. Adamczyk, T. Gucwa-Rys, A. Heczko, M. Kajetanowicz, G. Konopka-Cupiał, J. Majewski, W. Migdał, A. Misiak, and financial support by the Polish National Center for Development and Research through grant INNOTECH-K1/IN1/64/159174/NCBR/12, the Foundation for Polish Science through the MPD program, and the EU and MSHE Grant No. POIG.02.03.00-161 00-013/09.

Conflict of interest statement

Authors' conflict of interest disclosure: The authors stated that there are no conflicts of interest regarding the publication of this article. Research funding played no role in the study design; in the collection, analysis, and interpretation of data; in the writing of the report; or in the decision to submit the report for publication.
Research funding: None declared.
Employment or leadership: None declared.
Honorarium: None declared.

Received October 28, 2013; accepted January 30, 2014

References

1. Radon J. Ueber die Bestimmung von Funktionen durch ihre Integralwerte laengsbestimmter Mannigfaltigkeiten. Ber Verb Sächs Akad Wissensch Lepzig Math-Nat Kl 1917;69:262–77.
2. Herman GT. Image reconstruction from projections. New York: Academic Press, 1980.
3. Smith KT, Keinert F. Mathematical foundations of computed tomography. Appl Optics 1985;24:3950–7.
4. Parra L, Barrett H. List mode likelihood: EM algorithm and image quality estimation demonstrated on 2D PET. IEEE Trans Med Imag 1998;17:228–35.
5. Yokoi T, Shinohara H, Hashimoto T, Yamamoto T, Niio Y. Proceedings of the Second International Workshop on EGS, 8–12 August 2000, Tsukuba, Japan. KEK Proc 2000;20:224–34.
6. Wang ZA, Bovik C, Sheikh HR, Simoncelli EP. Image quality assessment: from error visibility to structural similarity. IEEE Trans Image Process 2004;16:600–12.